Log-Normal Melt Pulsation in Close-Coupled Gas Atomization

Andrew M. Mullis, Ian N. McCarthy and Robert F, Cochrane

Institute for Materials Research

University of Leeds

Leeds LS2-9JT, UK

Nicholas J. Adkins

IRC in Materials Processing,

The University of Birmingham

Edgbaston

Birmingham B15-2TT, UK

ABSTRACT

High speed photography coupled with sophisticated image analysis has been used to study low frequency pulsation during close-coupled gas atomization. At high gas pressure the instantaneous melt delivery is described by two superimposed log-normal distributions, one with a high standard deviation but little melt at the atomizer tip, the second with low standard deviation but more melt at the atomizer tip. At low gas pressures the distribution is better described by a single log-normal distribution.

Close-Coupled Gas Atomization (CCGA) is the production technique of choice when fine (5-50 μm), highly spherical, metal powders are required. In principle CCGA is straightforward, high pressure gas jets impinging upon a molten metal stream are used to disrupt the stream, breaking it into a spray of fine droplets. Liquid metal is delivered down the central bore of the nozzle, wherein it wets the nozzle tip (a process termed pre-filming, which is itself dependent upon the gas flow conditions) and is stripped off the circumferential edge of the nozzle by the gas. However, the complex interaction between the high velocity gas and the metal results in a turbulent, and often chaotic, flow with the result being that the details of the process are far from well understood. Consequently, early work into gas atomization focused on empirical correlations between median particle size and process parameters [1, 2] such as gas pressure, gas flow rate and melt flow rate. The most widely quoted of these empirical relationships is that due Lubanska [1], which correlates particle size with $(1+G)^{-1/2}$, where G is the gas:metal mass ratio.

For many potential powder metallurgy (PM) applications, both a small median particle size and a narrow size distribution in the product are desirable. While considerable progress has been reported on improving the efficiency with which the impinging gas jets disrupt the melt stream, and hence in reducing the median particle size [3, 4], most atomizer designs produce a distribution of powder sizes which span one order of magnitude or more [4]. As pointed out by Nasr et al. [5], remelting of the out of specification product can add substantially to the cost and energy usage of the overall process.

A number of factors contribute to this spread in the particle size distribution. In particular, common foundry experience is that close-coupled gas atomizers pulse, that is experience variations in the amount of metal being instantaneously delivered to the atomization tip, with this pulsation being in the frequency range 5-50 Hz. This is commonly seen as a flickering of the luminosity of the atomization spray cone, and has been quantitatively studied by applying Fourier analysis to high speed filming of the atomization process [6]. A significant scientific literature has built up attributing these fluctuations to the transition between open- and closed-wake conditions [6, 7 , 8]. Clearly, such pulsing of the melt causes

commensurate variations in the instantaneous gas:metal ratio and hence presumably in the size of the resulting powders.

The pulsatile model proposed by Ting et al. [7] suggests that during atomization in the closed-wake condition a dynamic balance exists between the momentum of the melt and the momentum of the atomizing gas. In gas only conditions, equilibrium is reached and the familiar pattern of shockwaves and flow features are established. The introduction of the liquid metal into the recirculation zone acts against the compressible gas, distorting and displacing these flow features. The changes in flow conditions causes the melt flow rate to slow or even stop, allowing the original flow features to re-establish. Once re-established melt is again able to flow into the recirculation zone and the cycle is re-established. However this is disputed by Mates and Settles [8, 9] who suggest that wake closure is of no real consequence in atomization as the closed-wake structure is not preserved during the actual atomization process.

In order to elucidate the nature of this pulsation behaviour imaging experiments were conducted on an analogue (water) atomizer and a research scale metal atomizer, both of which utilised an identical die of the discrete jet type with 18 cylindrical jets arranged around a tapered melt delivery nozzle with an apex angle of 45°. The design, which is shown schematically in Figure 1, is similar to the Ames HPGA-I [3] and USAG [10] designs. Although these designs are known to be sub-optimal in their atomization performance, the cylindrical jets giving rise to choked flow which limits the outlet gas velocity to Mach 1, we have used this geometry as it has been discussed extensively in the literature. Moreover, unlike the convergent-divergent jets used to produce supersonic gas flow, the simple cylindrical jet can be operated over a wide range of pressures, allowing the atomization process to be investigated as a function of pressure. Atomization experiments were conducted over inlet gas pressures in the range 0.5 - 5.5 MPa.

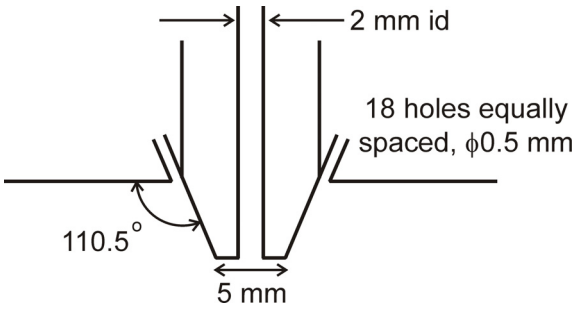

Figure 1. Schematic illustration of the geometry of the gas delivery die and melt nozzle used in the atomisation experiments.

For the metal atomization experiments a $Ni_{31.5}Al_{68.5}$ (Ni-50 wt.% Al) melt was used, with liquidus temperature of 1613 K (1340 °C). The melt was superheated by 200 K, giving a melt temperature prior to ejection of 1813 K (1540 °C). At this temperature the melt stream is sufficiently bright that filming can take place using the radiant light from the melt, even at high frame rates. Consequently, no external light sources were used. The melt was ejected from the guide tube under a constant overpressure of 40 kPa. Conversely, in the analogue atomization experiments imaging was performed in reflected light provided by two high power halogen lamps mounted in the base of the atomizer. Our previous high speed imaging studies [11, 12, 13] have shown that the analogue atomizer is a very good model for the metal atomizer, displaying many qualitatively similar phenomena including low frequency pulsation and high frequency precession of the second (atomized) fluid. In the context of the investigation conducted here performing experiments on an analogue atomizer has a number of advantages over performing metal atomization experiments, not least that the analogue atomizer can be run over a much wider range of gas inlet pressures, which is useful in elucidating the mechanism for the pulsation effect. Specifically, if the metal atomizer is run at too high a pressure (> 4.5 MPa) freeze-off of the melt at the atomization tip is a significant risk whereas if the metal atomizer is run at too low a pressure (< 1.5 MPa) incomplete atomization could result in a stream of hot metal pooling in the bottom of the chamber. In contrast, there are no issues associated with running the analogue atomizer in the pressure range 0.5 MPa ≤ P ≤ 5.5 MPa

Imaging of the melt spray cone was performed using a Kodak Ektapro 4540mx high speed digital motion analyzer, operating at 18,000 frames/s. The motion analyzer was fitted with high magnification optics which allowed full frame images (covering a distance ~5 cm from the die) to be imaged at a working distance of 25 cm. Frames were stored separately as high quality TIFF images without interlacing. The total recording time was 3.64 s.

One feature that is apparent from the filming, particularly when a number of images are combined into a movie, is that, as expected, there are considerable fluctuations in the amount of material being instantaneously delivered from the nozzle. These fluctuations, which are manifest in commensurate variations in the optical intensity at the tip, have been analysed quantitatively by taking a slice across each image. This slice is normal to the melt nozzle and 2 nozzle widths downstream of the nozzle outlet. The mean grey level intensity of the row of pixels within this slice is then calculated, giving a single statistic per frame which may be used as a proxy for the optical intensity of the melt instantaneously at the tip of the melt delivery nozzle, which may then be plotted as a time-sequence. As the grey level is recorded on an 8 bit scale this statistic varies from zero (no discernible melt is being discharged from the melt nozzle) to 255 (the pixels across the entire width of the frame in the slice are at saturation intensity). The lens aperture and camera gain are adjusted such that during peak discharge no pixels are at saturation brightness. From 3.64 s of filming at 18,000 frames/s, 65,536 such measurements of brightness at the tip are generated.

In a series of recent papers [11, 12] we have shown that if the Fourier transform of this average grey level time sequence is taken, two characteristic frequency regimes may be identified. A similar observation was made by Ting et al. [6] using a different methodology in which a 2-dimensional Fourier transform was applied to the whole image. The low frequency component of this oscillation, the majority of the spectral power of which is located < 50 Hz, is thought to be related to the pulsation behavior [6] of the melt

discharge which is the subject of the investigation here. Conversely, we have postulated that the high frequency variation, which generally has a well defined peak spectral power in the frequency range 300 - 1000 Hz (depending upon the atomization parameters and the thermophysical properties of the atomized fluid), is related to the motion of melt filaments within the spray cone. This observation appears to be confirmed by recent observations using ultra high speed (20 ns) pulsed laser imaging which has allowed the highly regular motion of such filaments to be observed directly [13]. However, as this high frequency variation in the optical intensity is related to the motion of the melt at the nozzle tip, and not to the quantity of melt present, this high frequency component of the signal is filtered out before we make any further analysis to understand the pulsation behavior of the melt.

In order to remove the high frequency components of the variation a low band pass filter is applied to the time-series data. For this we use a Butterworth IIR multi-section filter, as Butterworth filters are characterized by a magnitude response that is maximally flat in the pass-band and monotonic overall. The pass-band, with gain of 1 (0 db) is defined as the region $f \leq 60$ Hz, with an attenuation rising smoothly to -80 dB at a frequency of 300 Hz. This filter design is considered appropriate for the current application as those parts of the signal relating to melt pulsation (typically $f \leq 50$ Hz, and with negligible spectral power above 100 Hz) are preserved while components associated with motion of melt filaments (which have negligible spectral power below 200 Hz) are very effectively removed. The frequency transfer characteristics of the filter are shown in Figure 2, while the effect of applying the filter is shown in Fig. 3, in which we compare the raw and filtered time-series for a typical metal atomization experiment, in which the gas inlet pressure was 3.5 MPa.

The time averaged value of G, the gas-to-metal ratio, was measured during atomization at 2.84 (kg gas to kg melt). The median grey level is 30.58, with a minimum of 5.73 and a maximum of 68.98. On the assumption that (i) the gas flow rate is constant and (ii) that the measured and filtered grey level

corresponds directly to the volume of melt passing instantaneously through the measuring slice this would correspond to an equivalent variation in the instantaneous gas-to-metal ratio ranging from 1.26 (at grey level 68.98, maximum metal available at the tip) to 15.16 (at grey level 5.73, minimum metal available at the tip). Although no data is available relating the *instantaneous* gas-to-metal ratio to the size of the particles produced, in light of the well studied statistical correlations between *mean* gas-to-metal ratio and mass median particle size we would conjecture that such large variations in the instantaneous ratio are likely to be a significant contributory factor to the observed spread in the particle size distribution in gas atomized powders. The powder in this experiment had a mass-median diameter of 62.6 μm and like most gas atomized powders had a particle size distribution that followed a log-normal distribution. The (geometric) standard deviation in this particular case was 1.8.

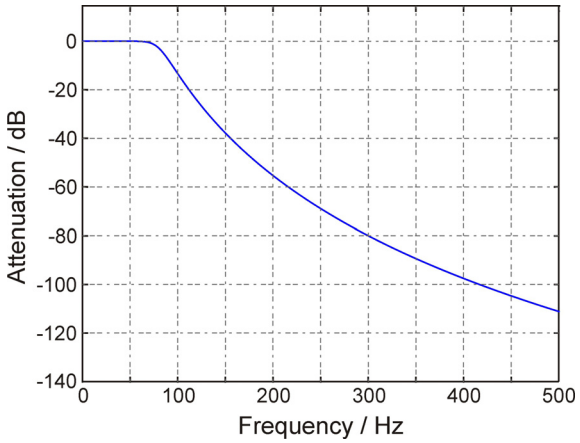

Figure 2. Frequency transfer characteristics of the Butterworth filter applied to the data. The filter has a gain of 1 (0 dB) between 0 and 60 Hz dropping to -80 dB at 300 Hz.

To explore the mechanism giving rise to pulsation at the tip $\log_{10}$-normal plots have been constructed by plotting the inverse normal probability function of the relative cumulative frequency against $\log_{10}$ of the intensity (grey) level. The result, shown in Fig. 4 for the time-series data depicted in Fig. 3, is that the data can be modeled as comprising of two segments, each of which is, to a good approximation, *log-*

normally distributed. At low optical intensities, corresponding to there being little metal at the atomization tip, the (geometric) standard deviation for the resulting distribution is 2.0. Conversely, at higher optical intensities, corresponding to there being more metal at the tip, the standard deviation is around 1.4.

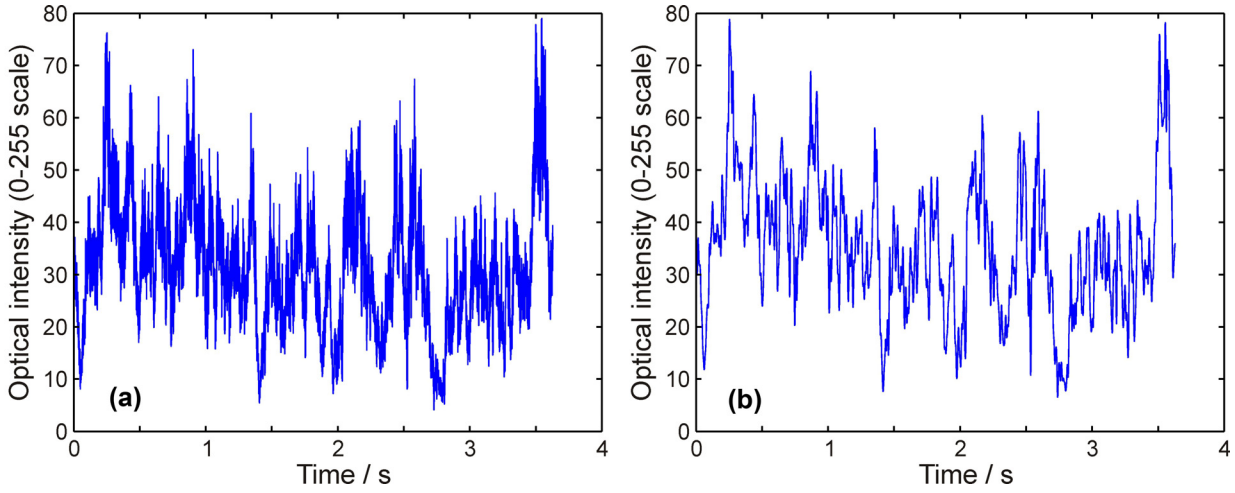

Figure 3. Time sequence showing the variation of optical intensity at the melt delivery nozzle tip (a) unfiltered and (b) after application of the Butterworth filter.

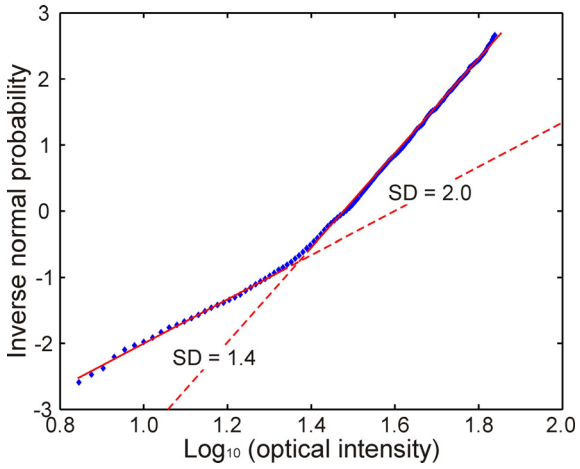

Figure 4. $\log_{10}$-normal frequency plot for the data shown in Figure 3 revealing the data follows two discrete log-normal distributions.

Figure 5 shows the inverse normal probability obtained from the cumulative frequency data plotted against $\log_{10}$(optical intensity) for the analogue atomizer running at two pressures, 1.75 MPa and 3.5 MPa. What is interesting is that at the lower pressure we observe a single log-normal distribution whereas at the higher pressure we observe two distinct distributions, as was the case for the metal atomizer. The geometric standard deviations for these are 1.2 at 1.75 MPa and 1.2 and 1.6 for the low and high standard deviation regimes at 3.5 MPa respectively. The pressure for this transition in behavior appears to be around 3.0 MPa, with atomization at low pressure always giving a single regime of log-normal behavior and atomization at high pressure giving two regimes of log normal behavior, with the higher standard deviation occurring for low melt flow.

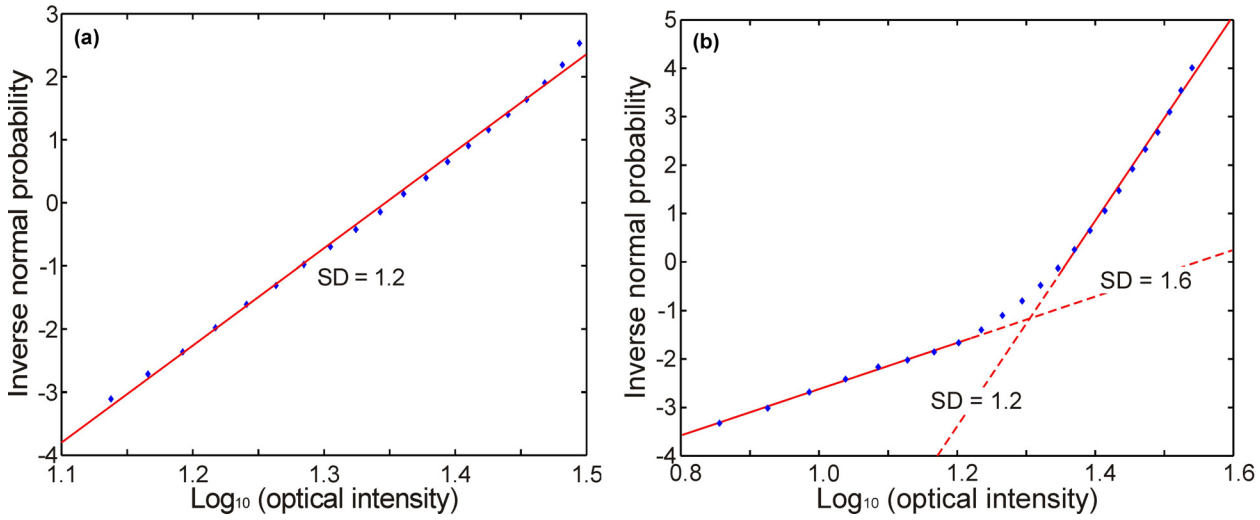

Figure 5. Log-normal plots for the analogue (water) atomizer operating at a gas pressure of (a) 1.75 MPa and (b) 3.5 MPa. At low pressure the intensity appears to follow a single log-normal distribution but at high pressure two distributions appear to be present, as was the case with the metal atomizer.

We note that the values of the standard deviation measured on the analogue atomizer appear to be significantly less than those measured during the atomization of Ni-Al melt. Specifically, taking the case

described above for atomization at high gas pressure, the standard deviation observed during the atomization of Ni-Al melt using radiant light from the melt at 1813 K (1540 °C) was 2.0 in the low flow regime and 1.4 in the high flow regime whereas the equivalent figures obtained using water as the analogue fluid in reflected light were 1.6 and 1.2 respectively. As the pulsation phenomenon is intimately linked to the momentum balance between the high pressure gas and the second fluid we suspect that the lower density of the analogue fluid, 1000 kg m^{-3} for water as opposed to 3750 kg m^{-3} for $Ni_{31.5}Al_{68.5}$ alloy at 1813 K (1540 °C) [14], is responsible for this. In deed, given the large difference in density we are gratified to observe qualitatively similar behavior between the metal and analogue systems.

The pulsation phenomenon in close-coupled gas atomizers is thought to arise due to the chaotic transition between open- and closed-wake conditions down-stream of the tip [6, 7]. However, it is also known that a minimum gas pressure is required to produce wake-closure and that below this pressure the wake will be permanently open. Ting et al. [7] reported the wake closure pressure in the system they studied as being around 4.0 – 4.5 MPa. Aspiration pressure measurements for the die/nozzle configuration used here [13] suggest that in this system wake closure occurs between 3.0 - 3.5 MPa. It is therefore tempting to speculate that the transition we observe here between the distribution of optical intensities being described by a single log-normal distribution and being described by two superimposed distributions is a consequence of the atomizer moving from being in the open-wake condition to being in the state where it is alternating between the open- and closed-wake conditions. If this is the case we could then also associate the two log-normal regimes observed at high gas pressure with the alternation between open- and closed-wake conditions, with the high flow rate, low standard deviation regime corresponding to the open-wake condition and the low flow rate high standard deviation regime corresponding to the close-wake condition.

In the case of metal atomization the crossover point between the two distributions occurs at an optical intensity of 23.5 (intersection of the two trend lines in Figure 4), which corresponds to the atomizer being

on the high standard deviation distribution around 25% of the time. However, because there is less metal at the tip during these times, this corresponds to significantly less than 25% of the product being produced during these periods. In fact, the fraction of product produced in this regime can be obtained by estimating the integral

$$\frac{\int_0^{23.5} I \cdot f \, dI}{\int_0^{255} I \cdot f \, dI}$$

where I is the intensity grey level and f the frequency density. Using this procedure we estimate around 14% of the total metal volume was discharged while the atomizer is in the high standard deviation state. The corresponding figures for the analogue atomizer are that it was in the high standard deviation state 21% of the time and that 16% of the total fluid volume was discharged during this time.

If the observed transition between high and low standard deviation behavior is related to the open- to closed-wake transition, the behavior observed here has significant implications for our understanding of the pulsation phenomenon in close-coupled gas atomization. In particular, it would appear that to claim that pulsation occurs due to the transition between open- and closed-wake conditions is overly simplistic. Rather, we observe that the atomizer transitions from an open-wake regime where it pulses with relatively low intensity to a closed-wake regime in which it pulses with much greater intensity. However, it is still the case that the closed-wake can be associated with low flow of material and that in all likelihood the ultimate cause of the pulsation is short timescale fluctuation in the aspiration conditions due to the chaotic interaction between the supersonic gas and the melt.

To visualize what this might mean in production we have plotted histograms of the variation of optical intensity observed in the analogue atomizer at 1.75 MPa and 3.5 MPa. In order to facilitate direct

comparison these have been plotted on the same axes, and the mean level has been subtracted from its respective distribution in each case. As a low optical intensity implies a small amount of liquid at the tip, and therefore a high ratio of gas to liquid, we might equate negative values on the x-axis to correspond to small droplet sizes and positive values to correspond to larger droplet sizes, although we would caution that this is unlikely to be a linear mapping. What is clear is that the optical intensity distribution, and therefore by inference the particle size distribution, has a significantly extended tail at the low intensity (small particle size) end of the distribution when operated above the wake closure pressure. Operating in this condition is likely therefore to result in the production of material that is very much finer than the median particle size. This is less likely to be the case when operating below the wake-closure pressure although, as suggested by [7], the atomization may be less efficient.

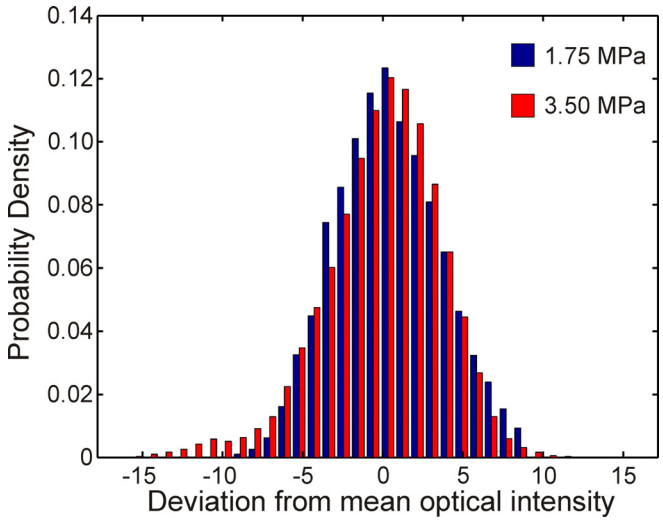

Figure 6. Comparison of the optical intensity distribution for the analogue atomizer run below and above wake-closure pressure.

1. H. Lubanska: J. Metals, 1970, vol. 22, pp. 45-49.
2. D. Bradley: J. Phys. D: Appl. Phys., 1973, vol. 6, pp. 1724-1736.
3. I.E. Anderson, R.S. Figliola and H. Morton: Mater. Sci. Eng., 1991, vol. 148A, pp. 101-114.
4. I.E. Anderson and R.L. Terpstra: Mater. Sci. Eng., 2002, vol. 326A, pp. 101-109.
5. G.G. Nasr, A.J. Yule, and L. Bendig, Industrial sprays and atomization design: Analysis and applications, Springer Publishing, 2002.
6. J. Ting, J. Connor and S. Ridder: Mater. Sci. Eng., 2005, vol. 390A, pp. 452-460.
7. J. Ting, M. Peretti and W.B. Eisen: Mater. Sci. Eng., 2002, vol. 326A, pp. 110-121.
8. S.P. Mates and G. S. Settles: Atomization and Sprays, 2005, vol. 15, pp. 41-59.
9. S.P. Mates and G.S. Settles: Atomization and Sprays, 2005, vol.15, pp. 19-40.
10. V. Anand, A.J. Kaufman, and N.J. Grant, in: R. Mehrabian, B.H. Kear and M. Cohen (eds.), Rapid Solidification Processing, Principles & Technologies II, Claitor, Baton Rouge, LA, 1978, pp. 273-286.
11. A.M. Mullis, N.J. Adkins, Z. Aslam, I.N. McCarthy and R.F. Cochrane: Int. J. Powder Metall., 2008, vol. 44, pp. 55-64.
12. I.N. McCarthy, Z. Aslam, N.J. Adkins, A.M. Mullis, and R.F. Cochrane: Powder Metall., 2009, vol. 52, pp. 205-212.
13. A.M. Mullis, I.N. McCarthy and R.F. Cochrane: J. Mater. Process Tech., 2011, vol. 211, pp. 1471-1477.
14. Intermetallic Materials Processing in Relation to Earth and Space Solidification (IMPRESS) Project (NMP3-CT-2004-500635) Deliverable Report D7.3.